Spin-Orbit-Free Topological Insulators without Time-Reversal Symmetry

A. Alexandradinata,[1] Chen Fang,[2,3,1] Matthew J. Gilbert,[4,3] and B. Andrei Bernevig[1]
[1]*Department of Physics, Princeton University, Princeton, New Jersey 08544, USA*
[2]*Department of Physics, University of Illinois, Urbana, Illinois 61801, USA*
[3]*Micro and Nanotechnology Laboratory, University of Illinois, 208 N. Wright Street, Urbana, Illinois 61801, USA*
[4]*Department of Electrical and Computer Engineering, University of Illinois, Urbana, Illinois 61801, USA*
(Received 14 March 2014; published 12 September 2014)

We explore the 32 crystallographic point groups and identify topological phases of matter with robust surface modes. For $n = 3, 4$, and 6 of the C_{nv} groups, we find the first-known 3D topological insulators without spin-orbit coupling, and with surface modes that are protected only by point groups; i.e., the relevant symmetries are purely crystalline and do not include time reversal. To describe these C_{nv} systems, we introduce the notions of (a) a halved mirror chirality, an integer invariant which characterizes half-mirror-planes in the 3D Brillouin zone, and (b) a bent Chern number, the traditional Thouless–Kohmoto–Nightingale–den Nijs invariant generalized to bent 2D manifolds. We find that a Weyl semimetallic phase intermediates two gapped phases with distinct halved chiralities. In addition to electronic systems without spin-orbit coupling, our findings also apply to intrinsically spinless systems such as photonic crystals and ultracold atoms.

DOI: 10.1103/PhysRevLett.113.116403 PACS numbers: 71.20.-b, 73.20.-r

Insulating phases are deemed distinct if they cannot be connected by continuous changes of the Hamiltonian that preserve both the energy gap and the symmetries of the phase; in this sense we say that the symmetry protects the phase. Distinct phases have strikingly different properties—of experimental interest are the presence of boundary modes, which in many cases distinguish a trivial and a topological phase. The symmetries that are ubiquitous in crystals belong to the space groups, and among them the point groups are the sets of transformations that preserve a spatial point. Despite the large number of space groups in nature, there are few known examples in which boundary modes are protected by crystal symmetries *alone* [1–4]. In this Letter, we explore the 32 crystallographic point groups and identify topological phases of matter with robust surface modes. For $n = 3, 4$, and 6 of the C_{nv} groups, we find the first-known 3D topological insulators (TIs) without spin-orbit coupling, and with surface modes that are protected only by point groups; our findings differ from past theoretical proposals [5–7] in not needing time-reversal symmetry (TRS). To describe these C_{nv} systems, we introduce the notions of (a) a *halved* mirror chirality, an integer invariant which characterizes half-mirror planes in the 3D Brillouin zone, and (b) a *bent* Chern number, the traditional Thouless—Kohmoto—Nightingale—den Nijs invariant [8] generalized to bent 2D manifolds (illustrated in Fig. 1).

To date, all experimentally realized TIs are strongly spin-orbit coupled, and a variety of exotic phenomenon originate from this coupling, e.g., Rashba spin-momentum locking on the surface of a TI [16]. Considerably less attention has been addressed to spinless systems, i.e., insulators and semimetals in which spin-orbit coupling is negligibly weak [4,5]. The topological classifications of spinless and spin-orbit-coupled systems generically differ. A case in point is SnTe, a prototypical C_{nv} system with strong spin-orbit coupling [2,17]. In SnTe, the mirror Chern number [1] was introduced to characterize planes in the 3D BZ which are invariant under reflection, or mirror planes in short. The Bloch wave functions in each mirror plane may be decomposed according to their representations under reflection, and each subspace may exhibit a quantum

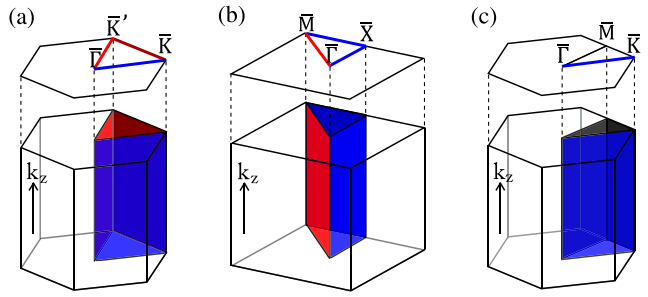

FIG. 1 (color online). Bottom: (a) Half-mirror-planes (HMPs) in the 3D Brillouin zone (BZ) of a hexagonal lattice with $C_{3v}^{(b)}$ symmetry. Blue face that projects to $\bar{\Gamma} - \bar{K}$: HMP_1. Brown, $\bar{K} - \bar{K}'$: HMP_2. Red, $\bar{\Gamma} - \bar{K}'$: HMP_3. (b) HMPs in the 3D BZ of a tetragonal lattice with C_{4v} symmetry. Red face that projects to $\bar{\Gamma} - \bar{M}$: HMP_4. Blue, $\bar{\Gamma} - \bar{X} - \bar{M}$: HMP_5. (c) Blue face that projects to $\bar{\Gamma} - \bar{K}$: HMP_1 in the 3D BZ of a hexagonal lattice with C_{6v} symmetry. Note that the black-colored submanifold in (c) is not a HMP. In each of (a),(b) and (c) we define a bent Chern number on the triangular pipe with its ends identified. Top: Nonblack lines are half-mirror lines (HMLs) in the corresponding 2D BZ of the 001 surface; each HML connects two distinct C_m-invariant points with $m > 2$.

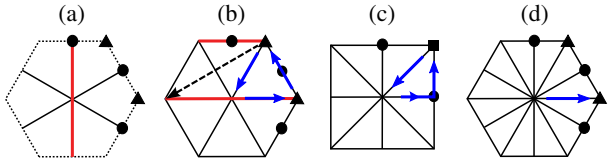

FIG. 2 (color online). (a) Top-down view of hexagonal BZ with $C_{3v}^{(a)}$ symmetry; our line of sight is parallel to the rotational axis. (b) Hexagonal BZ with $C_{3v}^{(b)}$ symmetry. (c) Tetragonal BZ with C_{4v} symmetry. (d) Hexagonal BZ with C_{6v} symmetry. Reflection-invariant planes are indicated by solid lines. Except the line through Γ, all nonequivalent C_n-invariant lines are indicated by circles for $n = 2$, triangles for $n = 3$, and squares for $n = 4$. For each of $\{C_{3v}^{(a)}, C_{3v}^{(b)}\}$, there are two independent mirror Chern numbers, defined as $\mathcal{C}_e$ ($\mathcal{C}_o$) in the mirror-even (odd) subspace [9]. In both (a) and (b), $\mathcal{C}_e$ and $\mathcal{C}_o$ are defined on a *single* mirror plane indicated in red; in (b), the two red lines correspond to two projected planes which connect through a reciprocal lattice vector (dashed arrow).

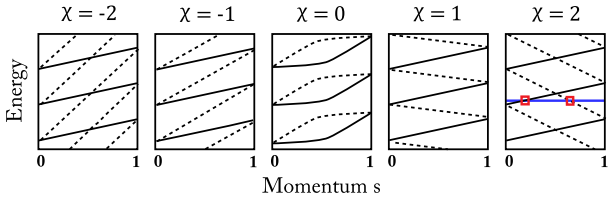

FIG. 3 (color online). Distinct connectivities of the (001) surface bands along the half-mirror lines. Black solid (dotted) lines indicate surface bands with eigenvalue $+1$ (-1) under reflection M_i; crossings between solid and dotted lines are robust due to reflection symmetry. For simplicity, we have depicted all degeneracies at momenta $s = 0$ and $s = 1$ as dispersing linearly with momentum. This is true if the little group of the wave vector (at $s \in \{0, 1\}$) is C_{3v}, but for C_{4v} and C_{6v} such crossings are in reality quadratic [9].

anomalous Hall effect [18]; we denote $\mathcal{C}_e$ ($\mathcal{C}_o$) as the Chern number in the even (odd) subspace of reflection. One may similarly define mirror Chern numbers for spinless C_{nv} systems, as illustrated for C_{3v} in Figs. 2(a) and 2(b). However, for $n = 2, 4$, and 6, such characterization is always trivial due to twofold rotational symmetry and the lack of spin-orbit coupling, i.e., $\mathcal{C}_e = \mathcal{C}_o = 0$ [9].

In this work, we propose that point-group-protected surface modes can exist without mirror Chern numbers, if the point group satisfies the following criterion: there exist at least two high-symmetry points (k_1 and k_2) in the surface BZ, which admit two-dimensional irreducible representations (irreps) of the little group [19] at each point. This is fulfilled by crystals with C_{4v} and C_{6v} symmetries, but not $\mathcal{C}_{2v}$. There exist in nature two kinds of C_{3v}: $C_{3v}^{(a)}$ and $C_{3v}^{(b)}$, which differ in the orientation of their mirror planes; compare Fig. 2(a) with Fig. 2(b). Only $C_{3v}^{(b)}$ fulfills our criterion. Henceforth, C_{nv} is understood to mean $C_{3v}^{(b)}$, C_{4v}, and C_{6v}. We are proposing that surface bands of C_{nv} systems assume topologically distinct structures on lines which connect $\boldsymbol{k}_1$ to $\boldsymbol{k}_2$. We are particularly interested in half-mirror lines (HMLs), that each satisfies two conditions. (a) It connects two *distinct* C_m-invariant points for $m > 2$; we illustrate this in Fig. 1, where a C_m-invariant point is mapped to itself under an m-fold rotation, up to translations by a reciprocal lattice vector. (b) All Bloch wave functions in a HML may be diagonalized by a *single* reflection operator. On these HMLs, we would like to characterize orbitals that transform in the 2D irrep of C_{nv}, e.g., (p_x, p_y) or (d_{xz}, d_{yz}) orbitals. We refer to these as the doublet irreps, and all other irreps are of the singlet kind.

We begin by parametrizing HML_i with $s_i \in [0, 1]$, where $s_i = 0$ (1) at the first (second) C_m-invariant point. The subscript i labels the different HMLs in a C_{nv} system; the ith HML is invariant under a specific reflection M_i. At $s_i = 0$ and 1, (001) surface bands form doubly degenerate pairs with opposite mirror eigenvalues, irrespective of whether the system has TRS. To prove this, let $U(g)$ represent the symmetry element g in the orbital basis. Suppose $U(M_i)|\eta\rangle = \eta|\eta\rangle$ for $\eta \in \{\pm 1\}$. By assumption, $|\eta\rangle$ transforms in the doublet representation; i.e., it is a linear combination of states with complex eigenvalues under $U(C_m)$, for $m > 2$. It follows that $[U(C_m) - U(C_m^{-1})]|\eta\rangle$ is not a null vector, and moreover it must have mirror eigenvalue $-\eta$ due to the relation $M_i C_m M_i^{-1} = C_m^{-1}$. Given these constraints at $s_i = 0$ and 1, there are $\mathbb{Z}$ ways to connect mirror-even bands to mirror-odd bands, as illustrated schematically in Fig. 3. We define the halved mirror chirality $\chi_i \in \mathbb{Z}$ as the *difference* in the number of mirror-even chiral modes with mirror-odd chiral modes; if $\chi_i \neq 0$, the surface bands robustly interpolate across the energy gap. χ_i may be easily extracted by inspection of the surface energy-momentum dispersion: first draw a constant-energy line within the bulk energy gap and parallel to the HML, e.g., the blue line in Fig. 3. At each intersection with a surface band, we calculate the sign of the group velocity dE/ds_i, and multiply it with the eigenvalue under reflection M_i. Finally, we sum this quantity over all intersections along HML_i to obtain χ_i. In Fig. 3, we find two intersections as indicated by red squares, and $\chi_i = (1)(1) + (-1)(-1) = 2$. The $\mathbb{Z}$ classification of (001) surface bands relies on doublet irreps in the surface BZ; on surfaces which break C_{nv} symmetry, the surface bands transform in the singlet irreps, and cannot assume topologically distinct structures.

Thus far we have described the halved chirality χ_i as a topological property of surface bands along HML_i, but we have not addressed how χ_i is encoded in the *bulk* wave functions. Taking $\hat{z}$ to lie along the rotational axis, each HML_i in the surface BZ is the $\hat{z}$ projection of a half-mirror plane (HMP_i) in the 3D BZ, as illustrated in Fig. 1. Each HMP connects two *distinct* C_m-invariant lines for $m > 2$, and all Bloch wave functions in a HMP may be diagonalized by a single reflection operator. HMP_i is parametrized by $t_i \in [0, 1]$ and $k_z \in (-\pi, \pi]$, where $t_i = 0$ (1) along the first

(second) C_m-invariant line. Then the halved mirror chirality has the following expression by bulk wave functions [9]

$$\chi_i = \frac{1}{2\pi}\int_{\mathrm{HMP}_i} dt_i dk_z (\mathcal{F}_e - \mathcal{F}_o) \in \mathbb{Z}. \quad (1)$$

For spinless representations, $M_i^2 = I$, and we label bands with mirror eigenvalue $+1$ (-1) as mirror-even (mirror-odd). $\mathcal{F}_e$ $(\mathcal{F}_o)$ is defined as the Berry curvature of occupied doublet bands [20,21], as contributed by the mirror-even (-odd) subspace.

For $C_{3v}^{(b)}$, there exists three independent HMPs as illustrated in Fig. 1(a), which we label by $i \in \{1,2,3\}$; all other HMPs are related to these three by symmetry. The C_{6v} group is obtained from $C_{3v}^{(b)}$ by adding sixfold rotational symmetry, which enforces $\chi_2 = 0$, and $\chi_1 = -\chi_3$. The sign in the last identity is fixed by our parametrization of $\{t_i\}$, which increase in the directions indicated by blue arrows in Fig. 2. Thus, HMP_1 is the sole independent HMP for C_{6v}. Finally, we find that there are two HMPs for C_{4v}, labeled by $i \in \{4,5\}$ [Fig. 1(b)]. Unlike the other highlighted HMPs, HMP_5 is the union of two mirror faces, HMP_{5a} and HMP_{5b}, which are related by a $\pi/2$ rotation. States in HMP_{5a} are invariant under the reflection $M_y : y \to -y$, while in HMP_{5b} the relevant reflection is $M_x : x \to -x$. The product of these orthogonal reflections is a π rotation (C_2) about $\hat{z}$, thus $M_x = C_2 M_y$. In the doublet representation, all orbitals are odd under a π rotation, thus $U(C_2) = -I$ and all states in HMP_5 may be labeled by a *single* operator $M_y \equiv M_5$.

The invariants $\{\chi_i\}$ are well defined so long as bulk states in the HMPs are gapped, which is true of C_{nv} insulators. These invariants may also be used to characterize C_{nv} semimetals, so long as the gaps close away from the HMPs. Such band touchings are generically Weyl nodes [22,23], though exceptions exist with a conjunction of time-reversal and inversion symmetries [24]. The chirality of each Weyl node is its Berry charge, which is positive (negative) if the node is a source (sink) of Berry flux. By the Nielsen-Ninomiya theorem, the net chirality of all Weyl nodes in the BZ is zero [25]. To make progress, we divide the BZ into "unit cells," such that the properties of one unit cell determine all others by symmetry. As seen in Fig. 1, these unit cells resemble the interior of triangular pipes; they are known as the orbifolds T^3/C_{nv}. The net chirality of an orbifold can be nonzero, and is determined by the Chern number on the 2D boundary of the orbifold. As each boundary resembles the surface of a triangular pipe, we call it a bent Chern number. We define $\mathcal{C}_{123}, \mathcal{C}_{45}$, and $\mathcal{C}_6$ as bent Chern numbers for $C_{3v}^{(b)}, C_{4v}$, and C_{6v}, respectively. $C_{3v}^{(b)}$ systems in the doublet representation are described by four invariants $(\chi_1, \chi_2, \chi_3, \mathcal{C}_{123})$, which are related by $\mathrm{parity}[\chi_1 + \chi_2 + \chi_3] = \mathrm{parity}[\mathcal{C}_{123}]$ [9]. If $\sum_{i=1}^3 \chi_i$ is odd, $\mathcal{C}_{123}$ must be nonzero due to an odd number of Weyl nodes within the orbifold, which implies the system is gapless. If the system is gapped, $\sum_{i=1}^3 \chi_i$ must be even. However, the converse is not implied. For C_{4v}, a similar relation holds: $\mathrm{parity}[\chi_4 + \chi_5] = \mathrm{parity}[\mathcal{C}_{45}]$ [9]. These parity constraints may be understood in light of a Weyl semimetallic phase that intermediates two gapped phases with distinct halved chiralities. There are four types of events that alter the halved chirality χ_i of HMP_i; we explain how Weyl nodes naturally emerge in the process. (i) Suppose the gap closes between two mirror-even bands in HMP_i. Around this band touching, bands disperse linearly within the mirror plane, and quadratically in the direction orthogonal to the plane. Within HMP_i, the linearized Hamiltonian around the band crossing describes a massless Dirac fermion in the even representation of reflection. If the mass of the fermion inverts sign, $\int_{\mathrm{HMP}_i} \mathcal{F}_e/2\pi$ changes by $\eta \in \{\pm 1\}$, implying that χ_i also changes by η through (1). This quantized addition of Berry flux is explained by a splitting of the band touching into two Weyl nodes of opposite chirality, and on opposite sides of the mirror face [Fig. 4(a)]. In analogy with magnetostatics, the initial band touching describes the nucleation of a dipole, which eventually splits into two opposite-charge monopoles; the flux through a plane separating two monopoles is unity. (ii) The same argument applies to the splitting of dipoles in the mirror-odd subspace, which alters $\int_{\mathrm{HMP}_i} \mathcal{F}_o/2\pi$ by $\kappa \in \{\pm 1\}$, and χ_i by $-\kappa$. For (iii) and (iv), consider two opposite-charge monopoles which converge on HMP_i and annihilate, causing χ_i to change by unity. The sign of this change

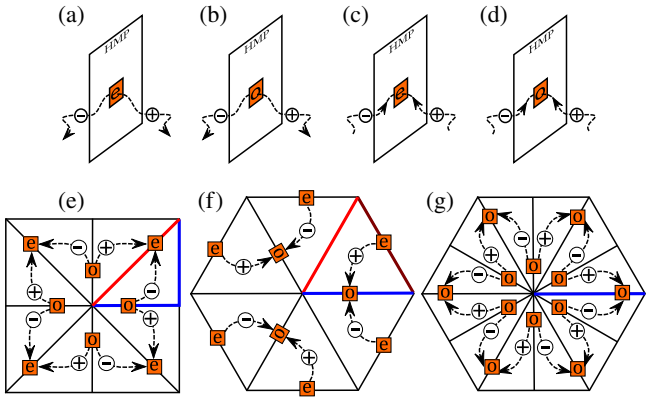

FIG. 4 (color online). (a)–(d) illustrate how the halved chirality of a HMP may change. The direction of arrows indicate whether Weyl nodes are created or annihilated. $+(-)$ labels a Berry monopole with positive (negative) charge; e (o) labels a crossing in the HMP between mirror-even (-odd) bands. (e)–(g) In three examples, we provide a top-down view of the trajectories of Weyl nodes, in the transition between two distinct gapped phases. Our line of sight is parallel to $\hat{z}$. Black lines indicate mirror faces, while colored lines specially indicate HMPs, with the same color legend as in Fig. 1. (e) describes a C_{4v} system, (f) $C_{3v}^{(b)}$, and (g) C_{6v}.

TABLE I. Topological classification of spinless insulators and semimetals with C_{nv} symmetry.

$C_{3v}^{(a)}$	$C_{3v}^{(b)}$	C_{4v}	C_{6v}
$\mathcal{C}_e, \mathcal{C}_o$	$\mathcal{C}_e, \mathcal{C}_o$	$\mathcal{C}_{45}$	$\mathcal{C}_6$
$\mathcal{C}_e, \mathcal{C}_o$	$\chi_1, \chi_2, \chi_3, \mathcal{C}_{123}$	$\chi_4, \chi_5, \mathcal{C}_{45}$	$\chi_1, \mathcal{C}_6$

is determined by whether the annihilation occurs in the mirror-even or -odd subspace. As modeled in the Supplemental Material [9], the transition between two distinct gapped phases is characterized by a transfer of Berry charge between two distinct HMPs [Figs. 4(e)–4(g)]. In the intermediate semimetallic phase, the experimental implications include Fermi arcs on the (001) surface [23,26,27].

We hope our classification stimulates a search for materials with C_{nv} symmetry. Why is C_{nv} special? We propose sufficient criteria for gapless surface modes whose robustness rely on a symmetry group. Minimally, (i) the symmetry must be unbroken by the presence of the surface. Additionally, either (ii) a reflection symmetry exists so that mirror subspaces can display a quantum anomalous Hall effect, or (iii) there exist at least two high-symmetry points in the surface BZ, which admit higher-than-one-dimensional irreps of the symmetry group. In addition to predicting new topological materials, these criteria are also satisfied by the well-known SnTe class, [2] and also the $\mathbb{Z}_2$ insulators [6,7,28–35]. Among the 32 crystallographic point groups, only the C_n and C_{nv} groups are preserved for a surface that is orthogonal to the rotational axis [19]. Though all C_{nv} groups satisfy (ii), the lack of spin-orbit coupling implies only $C_{3v}^{(a)}$ and $C_{3v}^{(b)}$ systems can have nonvanishing mirror Chern numbers [9]. While all C_n groups by themselves only have one-dimensional irreps, the C_4 or C_6 group satisfies (iii) in combination with TRS, as is known for the topological crystalline insulators introduced in Ref. [5]. Finally, only a subset of the C_{nv} groups possess two-dimensional irreps which satisfy (iii): $C_{3v}^{(b)}$, C_{4v}, and C_{6v}. In the second row of Table I, we list the topological invariants which characterize C_{3v}, C_{4v}, and C_{6v}, for bands of any irrep. In addition to the well-known mirror Chern numbers $(\mathcal{C}_e, \mathcal{C}_o)$, we have introduced the bent Chern numbers as a measure of the Berry charge in each orbifold T^3/C_{nv}. If the orbital character of bands near the gap is dominated by the doublet irreps, then the halved mirror chirality χ_i becomes a useful characterization, as seen in the third row of Table I. In particular, the mirror Chern numbers of $C_{3v}^{(b)}$ are completely determined by $(\chi_1, \chi_2, \chi_3, \mathcal{C}_{123})$ [9]. The singlet and doublet irreps of realistic systems are often hybridized. The topological surface bands that we predict here are robust, so long as this hybridization does not close the bulk gap, and if there are no errant *singlet* surface bands within the gap [5].

We discuss generalizations of our findings. In addition to materials whose full group is C_{nv}, we are also interested in higher-symmetry materials whose point groups reduce to C_{nv} subgroups in the presence of a surface, for $n = 3, 4$, or 6. We insist that these higher-symmetry point groups have neither (a) a reflection plane that is orthogonal to the principal C_n axis, nor (b) a twofold axis that lies perpendicular to the C_n axis, and parallel to the mirror plane. The presence of either (a) or (b) imposes $\chi = \mathcal{C}_e = \mathcal{C}_o = 0$ in any (half) mirror-plane of the C_{nv} system [9]. Only one such higher-symmetry point group exists: D_{3d} reduces to C_{3v} on the 111 surface [10]. Many C_{nv} systems naturally have TRS, which constrains all $C_{3v}^{(a)}$ and $C_{3v}^{(b)}$ invariants in Table I to vanish, with one independent exception for $C_{3v}^{(b)}$: $\chi_1 = -\chi_3$ can be nonzero [9]. TRS does not constrain the invariants of C_{4v} or C_{6v}. Our analysis of charge-conserving systems are readily generalized to spinless superconductors which are describable by mean-field theory. Because of the particle-hole redundancy of the mean-field Hamiltonian, the only nonvanishing invariants from Table I belong to $C_{3v}^{(a)}$ and $C_{3v}^{(b)}$; among these nonvanishing invariants, the only constraint is $\chi_1 = \chi_3$ for $C_{3v}^{(b)}$ [9]. While we have confined our description to electronic systems without spin-orbit coupling, the halved chirality is generalizable to photonic crystals which are inherently spinless, and also to cold atoms. Finally, we point out that the bent Chern number and the halved chirality are also valid characterizations of spin-orbit-coupled systems with mirror symmetry. In particular, (1) applies to representations with spin if we redefine the mirror-even (-odd) bands as having mirror eigenvalues $+i$ $(-i)$ [9]. The implications are left to future work.

A. A. is grateful to Yang-Le Wu and Tim Lou for insightful interpretations of this work. A. A. and B. A. B. were supported by the Packard Foundation, 339-4063–Keck Foundation, NSF CAREER DMR-095242, ONR-N00014-11-1-0635, and NSF-MRSEC DMR-0819860 at Princeton University. This work was also supported by DARPA under SPAWAR Grant No. N66001-11-1-4110. C. F. is supported by ONR-N0014-11-1-0728 and DARPA-N66001-11-1-4110. M. J. G. acknowledges support from the ONR under Grants No. N0014-11-1-0728 and No. N0014-14-1-0123, and the Center for Advanced Study (CAS) at the University of Illinois.

[1] J. C. Y. Teo, L. Fu, and C. L. Kane, Phys. Rev. B **78**, 045426 (2008).
[2] T. H. Hsieh, H. Lin, J. Liu, W. Duan, A. Bansi, and L. Fu, Nat. Commun. **3**, 982 (2012).
[3] S.-Y. Xu *et al.*, Nat. Commun. **3**, 1192 (2012).
[4] C.-X. Liu and R.-X. Zhang, arXiv:1308.4717.
[5] L. Fu, Phys. Rev. Lett. **106**, 106802 (2011).
[6] R. Roy, Phys. Rev. B **79**, 195321 (2009).
[7] L. Fu and C. L. Kane, Phys. Rev. B **74**, 195312 (2006).

[8] D. J. Thouless, M. Kohmoto, M. P. Nightingale, and M. den Nijs, Phys. Rev. Lett. **49**, 405 (1982).
[9] See Supplemental Material at http://link.aps.org/supplemental/10.1103/PhysRevLett.113.116403, which provides models of various topological phases described in this Letter, as well as more technical formulations of the associated topological invariants; the Material makes reference to Refs. [10–15].
[10] G. F. Koster, *Properties of the Thirty-Two Point Groups* (MIT Press, Cambridge, MA, 1963).
[11] J. Slater and G. Koster, Phys. Rev. **94**, 1498 (1954).
[12] C. M. Goringe, D. R. Bowler, and E. Hernandez, Rep. Prog. Phys. **60**, 1447 (1997).
[13] P. Lowdin, J. Chem. Phys. **18**, 365 (1950).
[14] R. D. King-Smith and D. Vanderbilt, Phys. Rev. B **47**, 1651 (1993).
[15] A. Alexandradinata, X. Dai, and B. A. Bernevig, Phys. Rev. B **89**, 155114 (2014).
[16] R. Winkler, *Spin-Orbit Coupling Effects in Two-Dimensional Electron and Hole Systems*, Springer Tracts in Modern Physics (Springer, New York, 2003).
[17] Y. Tanaka, Z. Ren, T. Sato, K. Nakayama, S. Souma, T. Takahashi, K. Segawa, and Y. Ando, Nat. Phys. **8**, 800 (2012).
[18] F. D. M. Haldane, Phys. Rev. Lett. **61**, 2015 (1988).
[19] M. Tinkham, *Group Theory and Quantum Mechanics* (Dover, New York, 2003).
[20] M. V. Berry, Proc. R. Soc. A **392**, 45 (1984).
[21] J. Zak, Phys. Rev. Lett. **48**, 359 (1982); **62**, 2747 (1989).
[22] S. Murakami, New J. Phys. **9**, 356 (2007).
[23] X. Wan, A. M. Turner, A. Vishwanath, and S. Y. Savrasov, Phys. Rev. B **83**, 205101 (2011).
[24] A. A. Burkov, M. D. Hook, and L. Balents, Phys. Rev. B **84**, 235126 (2011).
[25] H. B. Nielsen and M. Ninomiya, Nucl. Phys. **B185**, 20 (1981).
[26] G. B. Halasz and L. Balents, Phys. Rev. B **85**, 035103 (2012).
[27] C. Fang, M. J. Gilbert, X. Dai, and B. A. Bernevig, Phys. Rev. Lett. **108**, 266802 (2012).
[28] C. L. Kane and E. J. Mele, Phys. Rev. Lett. **95**, 226801 (2005).
[29] C. L. Kane and E. J. Mele, Phys. Rev. Lett. **95**, 146802 (2005).
[30] B. A. Bernevig and S. C. Zhang, Phys. Rev. Lett. **96**, 106802 (2006).
[31] B. A. Bernevig, T. L. Hughes, and S. C. Zhang, Science **314**, 1757 (2006).
[32] M. König, S. Wiedmann, C. Brüne, A. Roth, H. Buhmann, L. Molenkamp, X.-L. Qi, and S.-C. Zhang, Science **318**, 766 (2007).
[33] L. Fu, C. L. Kane, and E. J. Mele, Phys. Rev. Lett. **98**, 106803 (2007).
[34] J. E. Moore and L. Balents, Phys. Rev. B **75**, 121306 (2007);
[35] D. Hsieh, D. Qian, L. Wray, Y. Xia, Y. S. Hor, R. J. Cava, and M. Z. Hasan, Nature (London) **452**, 970 (2008).